eNeurologicalSci 22 (2021) 100314

Contents lists available at ScienceDirect

eNeurologicalSci

journal homepage: www.elsevier.com/locate/ensci

Functional connectivity of the motor system in dystonia due to PKAN

Peter Stoeter [a,*], Pedro Roa [b], Pamela Bido [b], Herwin Speckter [a], Jairo Oviedo [a], Rea Rodriguez-Raecke [c]

[a] Department of Radiology, CEDIMAT, Santo Domingo, Dominican Republic
[b] Department of Neurology, CEDIMAT, Santo Domingo, Dominican Republic
[c] Brain Imaging Facility, IZKF Aachen, RWTH Aachen University, Aachen, Germany

ARTICLE INFO

Keywords:
Pantothenate Kinase Associated
Neurodegeneration
Dystonia
Resting state
Functional connectivity

ABSTRACT

Purpose: To demonstrate deviations of functional connectivity within the motor system in dystonic patients suffering from Pantothenate Kinase Associated Neurodegeneration, a genetic and metabolic disease, which is characterized by a primary lesion in the globus pallidus.

Material and methods: Functional Magnetic Resonance Imaging data were measured during resting state in 12 patients suffering from a confirmed mutation of the PANK2 gene. In this region-of-interest based analysis, data were evaluated in respect to correlation of signal time course between basal ganglia, motor-related cortical regions and cerebellum, were related to clinical data and were compared to a control group of 20 healthy volunteers.

Results: During resting state, correlation coefficients within the motor system were significantly lower in patients than in controls (0.025 vs. 0.133, $p < 0.05$). Network analysis by Network Based Statistics showed that these differences mainly affected the connectivity between a sub-network consisting of the basal ganglia and another one, the motor system-related cortical areas ($p < 0.05$). 6 out of 12 connections, which correlated significantly to duration of disease, were connections between both sub-networks.

Conclusion: The finding of a reduced functional connectivity within the motor network, between the basal ganglia and cortical motor-related areas, fits well into the concept of a general functional disturbance of the motor system in PKAN.

1. Introduction

Pantothenate Kinase Associated Neurodegeneration (PKAN) is the most frequent entity of diseases grouped under the term of Neurodegeneration with Brain Iron Accumulation, formerly known as Hallervorden-Spatz disease [1]. PKAN is an autosomal-recessive disorder. With an estimated prevalence of 1:1,000,000, it belongs to the "Rare Diseases". The responsible mutation has been localized to the PANK2 gene on the chromosomal position 20p13. The resulting metabolic defect affects the formation of one of the four different varieties of pantothenate kinase. These enzymes regulate the production of coenzyme A from vitamin B5 and are involved in energy and lipid metabolism [2].

In the "classical" form of PKAN, the onset of symptoms is early in childhood and runs a progressive course. In about one quarter of cases however, the disease starts atypically late during teenage years or early adulthood, followed by slower progression, and there are intermediate cases. The clinical manifestation is variable and mainly characterized by dystonic movements affecting the oro-pharyngeal or cervical area, the trunk or extremities. Parkinsonian features have been described in older patients as well as impulsive behavior and pigmentary retinopathy [3].

Pathological changes mainly affect the globus pallidus with variable involvement of neighboring parts of the basal ganglia as the subthalamic nucleus or the substantia nigra, whereas the cortex, most parts of the brainstem and the rest of the central grey matter is not involved [4]. In Magnetic Resonance Imaging (MRI), the "eye-of-the-tiger"-sign is regarded as the classical finding confirming the presence of PKAN [5]. In T2- and T2 star weighted imaging, it consists of a bright spot in the antero-medial part of the globus pallidus surrounded by a dark area covering the posterior parts of this nucleus. The bright spot represents an area of gliosis and has been reported to appear before the surrounding accumulation of extracellular iron is evident [6]. The accumulation of

* Corresponding author at: Department of Radiology, CEDIMAT, Plaza de la Salud, Santo Domingo, Dominican Republic.
E-mail address: peter.stoeter@gmx.de (P. Stoeter).

https://doi.org/10.1016/j.ensci.2021.100314
Received 29 May 2020; Received in revised form 30 November 2020; Accepted 17 January 2021
Available online 19 January 2021

Table 1
Patients and controls, personal and clinical data.

	n, gender	Age (years)	Age of onset	Duration	Dystonia scale	Disability scale
Patients	12, 7 f:5m	18.9 (6.6–33.9)	9.3 (5–15)	7.9 (0.5–23)	28.8 ± 25.1	10.7 ± 9.1
Controls	20, 11 f:9m	19.2 (8.7–30.7)				

iron increases with age, but without clear relation to the severity of the dystonia [7].

In functional MRI motor activation studies, patients showed a larger amount of activated voxels in the contralateral premotor cortex, SMA and primary motor cortex before and in the contralateral putamen at the time of the actual hand movement, which correlated positively to the degree of dystonia affecting the contralateral arm [8].

According to these neuropathological and MRI findings, globus pallidus is the main nucleus of the basal ganglia to be affected, and the hypothesis of a reduction of its inhibitory input to the motor nucleus of the thalamus is in line with the traditional pathophysiologic concept of the origin of dystonic movements in PKAN [9]. Recent tractography and magneto-encephalographic studies have shown evidence for further, direct and mono- or polysynaptic connections between cortical areas, basal ganglia and cerebellum, where among others, a sensorimotor-pallidal pathway could play an important role in motor control [10].

By examination of functional connectivity between various subcomponents of this network, we expect to see differences between dystonic patients and controls that possibly mirror their movement disorder. Our functional Magnetic Resonance Imaging (MRI) Region-of-interest (ROI) based study is the first one to look into connectivity within the motor network in PKAN dystonia by analyzing resting state activity in motor-related areas in a group of genetically confirmed patients living in the Dominican Republic [11].

2. Material and methods

The study had been approved by the local Ethics Committee, and informed consent had been received from all participants.

2.1. Patients and controls

Included were 12 patients with genetically confirmed PKAN dystonia with an age range from 6.6 to 33.9 years (mean: 18.9 years), 7 females and 5 males, and an age-matched control group of 20 healthy volunteers without any family relations to the patients (8.7 to 30.7 years, mean age 19.2 years, 11 females and 9 males) (Table 1). In our sample were no patients of the classic early onset type before the age of 6 years. 5 patients showed an intermediate onset between 6 and 10 years and 7 a late onset after 10 years of age. At the time of MRI examination, patients had been suffering from PKAN from 0.5 to 23 years (mean: 7.9 years). Dystonic symptoms affected extremities and trunk. Most cases also showed oro-pharyngeal involvement, and the older patients displayed some Parkinsonian symptoms like freezing. Scoring on the Burke-Fahn-Marsden (BMF) Scale was between 1 and 69.5 points (mean: 28.9 points) and 2 to 26 points (mean: 10.7 points) on the disability scale. Apart from occasional analgesics and tranquillizers, there was no specific therapy in 10 patients. Two of them however participated in an open-label Phosphopantothenate Replacement trial, which resulted in slowing down progression of symptoms, but without changing the clinical expression of dystonia [12].

Main inclusion criteria in volunteers as well as in patients –apart from their genetic findings and showing the "tiger's eye" in patients- were the relative absence of movement artifacts in the functional MRI study, defined by the number of "scrubbed frames" (see below).

2.2. MR examination

MR examinations were carried out on a 3 T Achieva scanner (Philips):

- T2W Sequence: TR/TE = 2050/80 ms, 25 transversal slices, thickness 5 mm,
- T1W Gradient Echo Sequence: TR/TE = 6.73/3.11 ms, 180 sagittal slices, voxel size 1 mm^3
- EPI-Gradient Echo Sequence: TR 2 s, 34 slices of 3 mm thickness providing full brain coverage, gap 0.75 mm, FOV 192 mm, voxel size 2.38 × 2.38 × 3 mm, 300 dynamics over 10 min. To achieve resting state conditions during this measurement, subjects were requested to lie quiet in the scanner with eyes closed thinking of nothing special but to let their minds wander around.

Table 2
ROIs and their x, y and z center coordinates used for measurement of resting state connectivity within the motor system.

Area	Left			Right		
Caudatum	−14	15	6	14	15	6
Putamen	−28	4	2	28	4	2
Globus Pallidus	−22	−4	2	22	−4	2
Precentral Gyrus	−52	−12	46	52	−12	46
Postcentral Gyrus	−44	−27	50	44	−27	50
Dorsal Premotor Area	−32	2	60	32	2	60
Ventral Premotor Area	−48	4	24	48	4	24
Pre-SMA	−6	10	60	6	10	60
SMA	−8	−12	62	8	−12	62
Superior Part of Cerebellum	−10	−54	−18	8	−50	−16

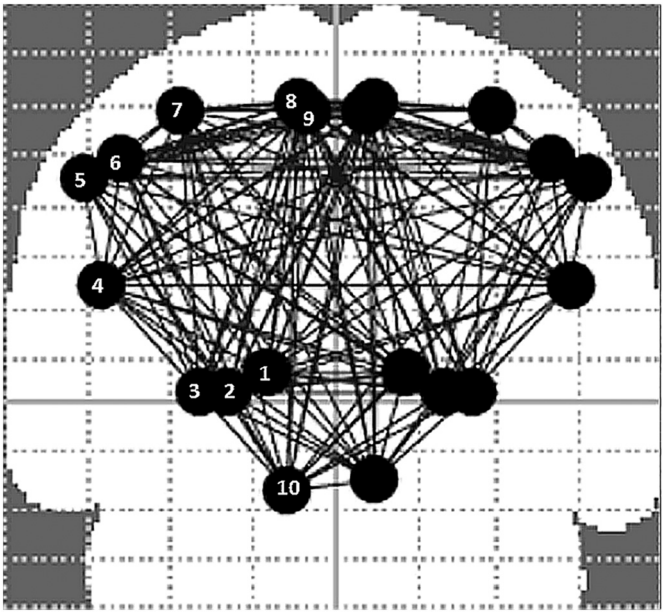

Fig. 1. Glass-brain presentation, ap-view, of ROIs included into evaluation. 1: Caudatum, 2: Putamen, 3: Globus pallidus, 4: Ventral Premotor Area, 5: Precentral Gyrus, 6: Postcentral Gyrus, 7: Dorsal Premotor Area, 8: SMA, 9: Pre-SMA, 10: Superior Part of Cerebellum.

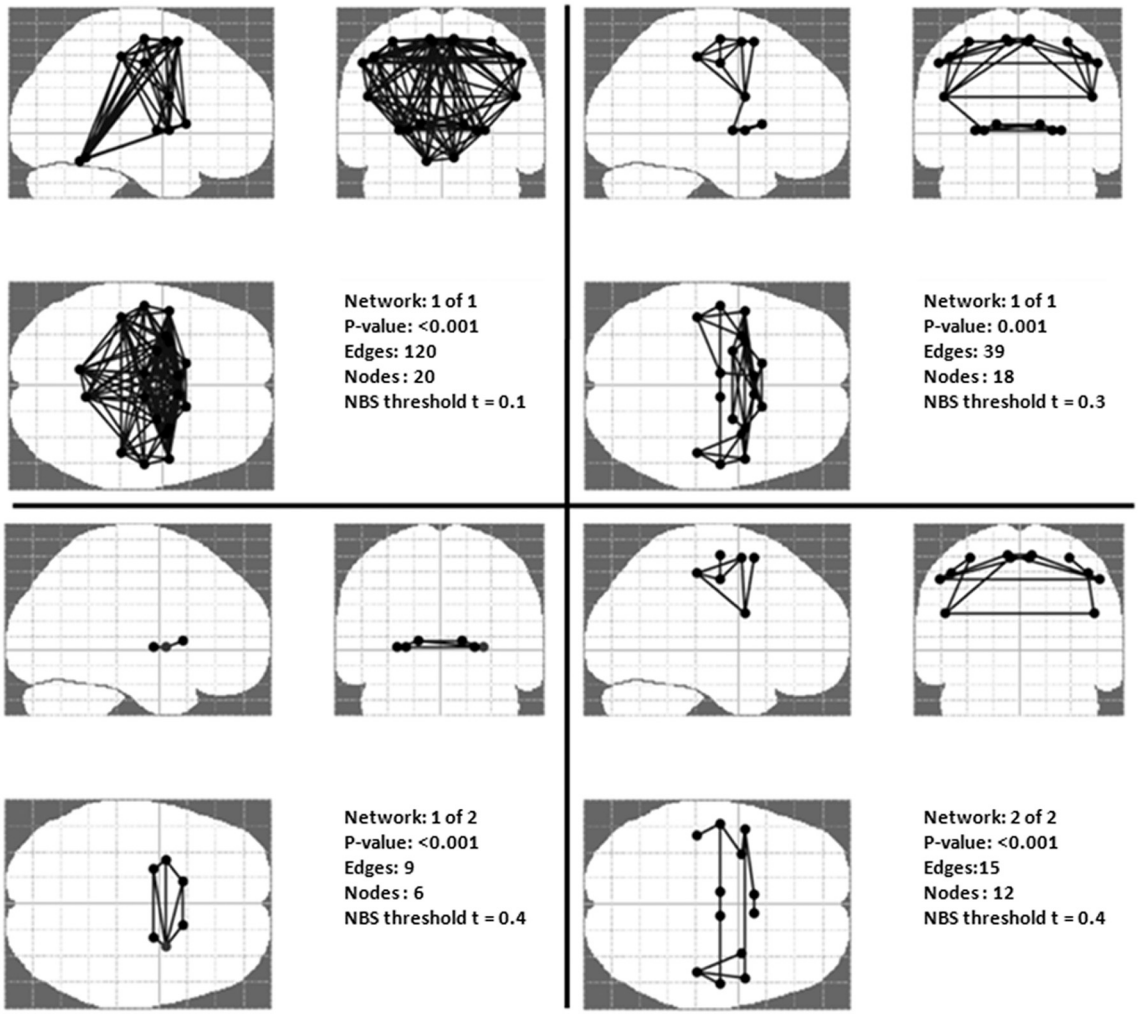

Fig. 2. NBS one-sample *t*-test results identifying networks in group of patients (a) and controls (b) at thresholds of $t = 0.1$ (upper image left), $t = 0.3$ (upper image right) and $t = 0.4$ (lower images left and right). In patients and controls, at lower thresholds, one common network is identified, however with fewer edges in patients. The difference between patients and controls is most evident for edges between the upper and lower network components at a threshold of $t = 0.3$ (1 edge in patients and 7 edges in controls, compare upper right images in (a) and (b)). At a threshold of $t = 0.4$, both components appear as separate sub-networks in patients and controls.

2.3. *Postprocessing of data*

Image processing was performed with Statistical Parametric Mapping (SPM12, www.fil.ion.ucl.ac.uk/spm) and included slice timing, realignment and spatial normalization. To define ROIs, we used the Human Area Template atlas from the University of Illinois published by Mayka et al [13], which contains 12 cortical and 10 subcortical areas related to the motor system (Table 2). In order to avoid ROIs of a size below 2.5 cm^3, we combined the masks of the internal and external globus pallidus to a common globus pallidus, and replaced the masks of the subthalamic nucleus by the superior parts of the cerebellum taken from the Stanford atlas [14], which include the upper third of the vermis and the adjacent part of the left or right hemisphere. Altogether, 20 ROIs were included (see Table 2 and Fig. 1).

The regional parcellations were first co-registered to the MNI T1 2 mm brain template and thereafter to the T2 gradient echo mean images using affine linear registration as included in the FSL software package (FSL 5.0 FLIRT, http://fsl.fmrib.ox.ac.uk/fsl/fslwiki).Without smoothing of data, signal intensities of all voxels in one region were averaged for each time point, followed by regressing out head movement parameters (six parameters, calculated during the movement correction step), cerebrospinal fluid (CSF) signals, and white matter signals (both extracted from a 5 mm spherical ROI using Marsbar Toolbox 0.43, http://marsbar.sourceforge.net/) [15]. In spite of some concern of "artifactual" introduction of spurious anti-correlations [16], we also applied global signal regression to remove sources of global variance such as respiration and head movements. Framewise displacement was calculated as the sum of absolute values of the derivatives of the 6 realignment parameters, and as suggested by Power et al. [17], frames presenting values below 0.5 were discarded from further data evaluation. The number of "scrubbed" frames was not significantly different between both groups (mean in patients 12.1, mean in controls 9.7, $p > 0.5$). The procedure has been described in detail before [18].

From the resulting region-averaged time series, we created a functional connectivity matrix by calculating the Pearson correlation between all selected ROIs related to the motor system. The resulting Correlation Coefficients (CCs) were compared by 2-tailed *t*-test between groups. CCs of patients were correlated to their clinical data (age at onset and duration of symptoms and severity of dystonia and disability according to the BFM scale) by Pearson's correlation, corrected for age, using the SSPS statistical package (www.ibm.com/de-de/analytics/spss-statistics-software). Significance was accepted at a 95% level

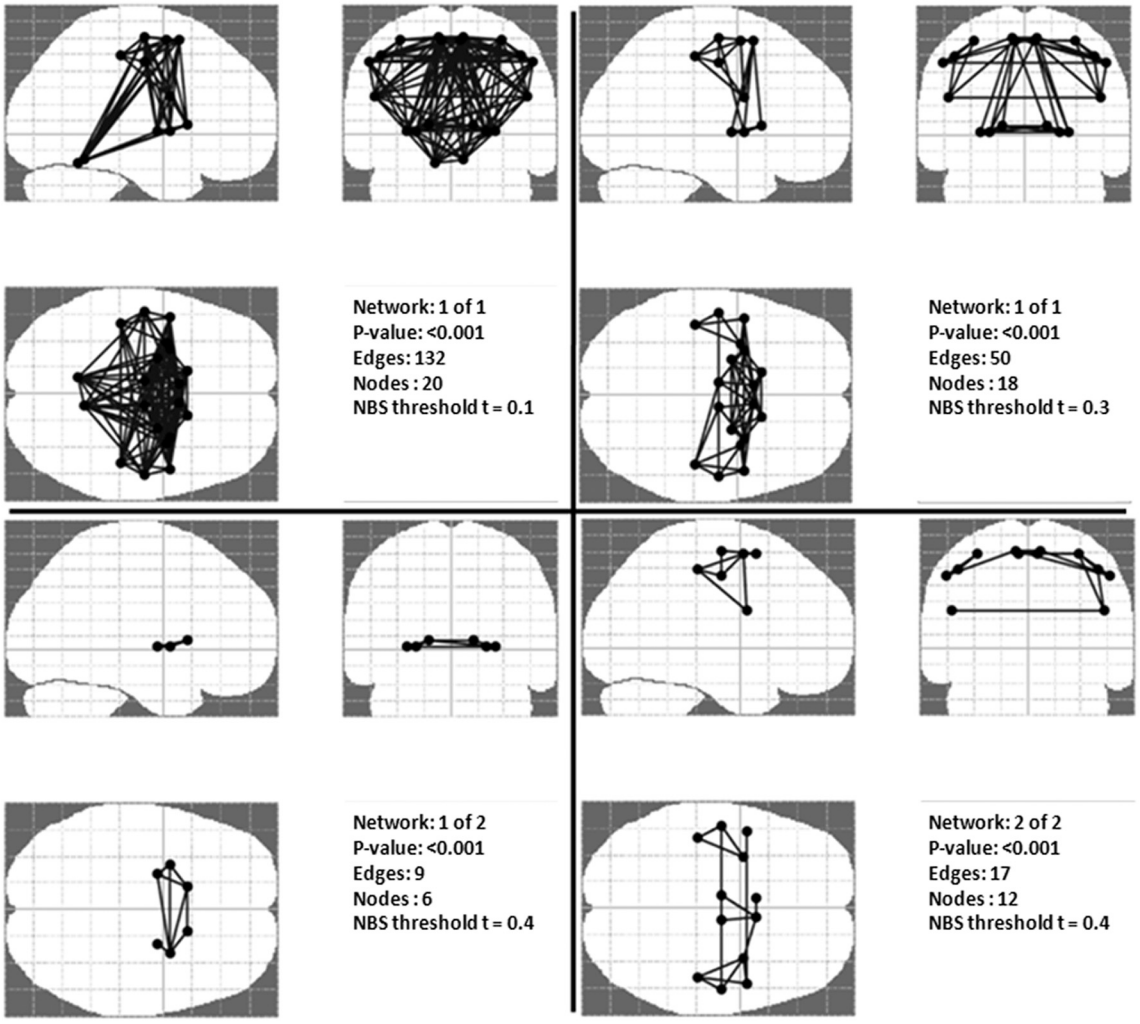

Fig. 2. (*continued*).

after False Detection Rate (FDR) correction for multiple comparisons (www.sdmproject.com/utilities/?show=FDR).

To identify sub-components of motor network connections within groups of patients and controls, and to look for differences between groups and also for correlation to clinical data, we used Network based Statistics (NBS, www.nitrc.org/projects/nbs), which uses the correlation matrices described above and corrects for multiple comparison and allows higher dimensional analysis rather than the Independent Component Analysis and simple seed-based correlation analysis. NBS controls for multiple comparisons through cluster-based thresholding, in which connected components of a network are considered a cluster [19].

Here, within-group analysis was carried out by one-sample *t*-test applied to individual CC matrices and by two-tailed *t*-test comparing 6 patients below and 6 patients above the age of 15 years, comparison between groups by two-tailed *t*-test, and an analysis of covariance of patients' data to clinical parameters as age at onset and duration of disease, severity of dystonia and disability according to the BFM scale, all corrected for age at examination. The latter parameter was introduced as nuisance covariate. Calculations were performed with 5000 permutations each, flipping the sign of each data point for each mutation, at a significance level initially set to $p < 0.05$. Measurement of significance was based on the number of connections ("edges") between ROIs ("nodes"), the "extent", which is supposed to disclose relative weak effects including many connections. Initially, relative low cluster-defining primary test statistic thresholds 0.1 to 0.4 were used to identify suprathreshold edges within-group sub-networks. As has been described before [20], comparison between groups and correlation to clinical data was carried out at various higher thresholds of 2.2 to 2.6 and 8.2 to 9.2 respectively. These thresholds corresponded to the highest range where the sub-networks identified before were still displayed.

3. Results

3.1. Group-specific correlations between motor-related areas

During resting state, the means of all CCs between all ROIs of the motor system were significantly lower in patients than in controls (0.025 vs. 0.133, $p < 0.05$). However, when CCs between two individual ROIs were compared separately between groups, no such difference reached significance after FDR correction.

Group-specific NBS evaluation of the CC matrices, confined to patients and confined to controls, gave similar results in both groups (see Fig. 2a and b): at the threshold of $t = 0.1$, one common motor network appeared in both groups with all 20 ROIs named "nodes" including the cerebellum. However, due to the level of significance set to $p < 0.05$, fewer edges appeared in patients (120 vs. 132).

At a higher threshold of $t = 0.3$, the nodes of the cerebellum respective their edges were no longer included in both groups, and the number of edges between the remaining 18 nodes was lowered to a larger extent in patients (to 39) than in controls (to 50). This reduction of edges affected mainly the connections between the cortical ROIs and the basal ganglia (1 remaining edge in patients and 8 remaining edges in

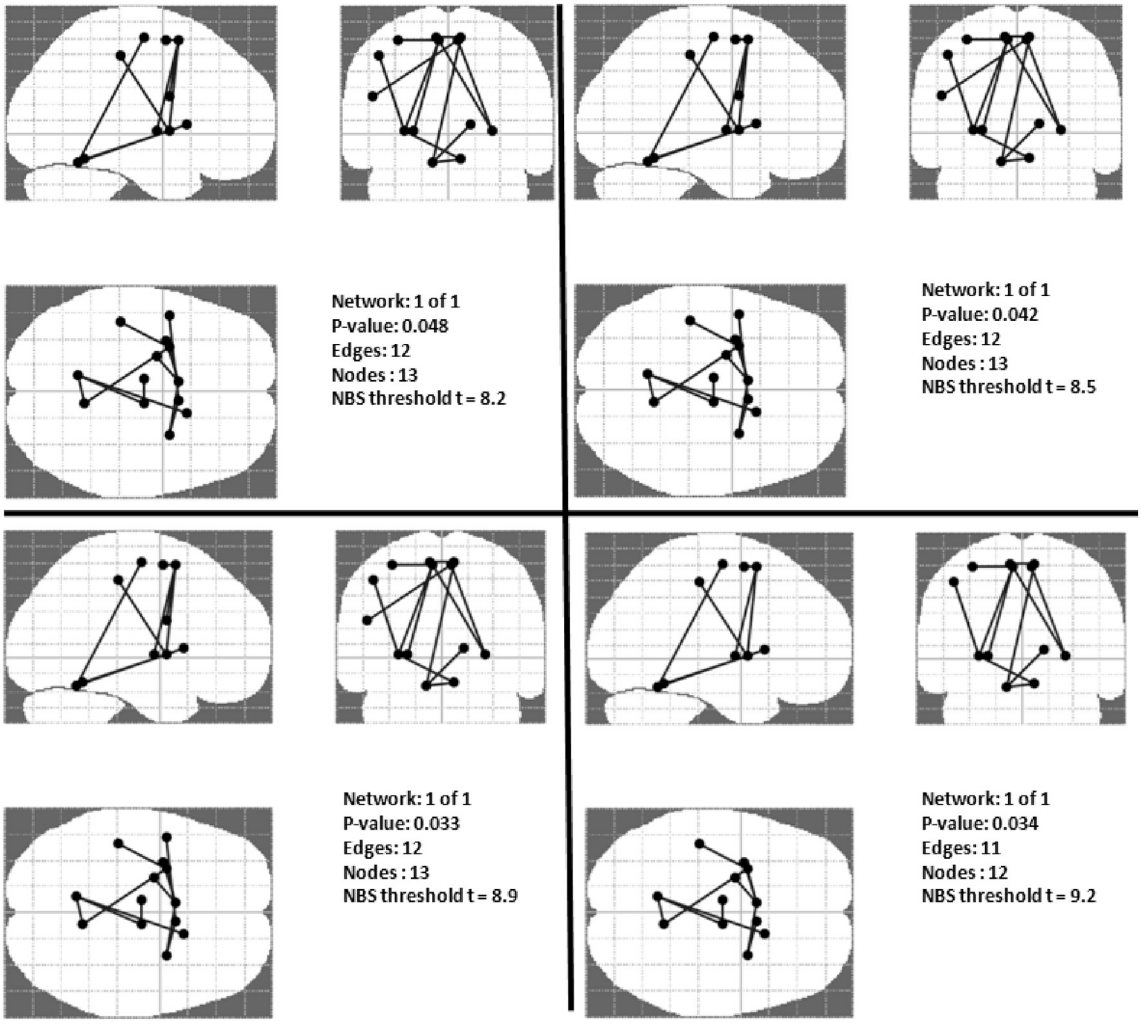

Fig. 3. NBS ANOVA results in patients, which relate correlations between ROIs of the motor system to duration of symptoms. At a threshold of $t = 8.2$ (upper image left), 12 edges are identified with a significant ($p < 0.05$) negative correlation to duration of symptoms, 5 of them are localized between basal ganglia and cortical motor-related areas. At a threshold of $t = 9.2$ (lower image right), 11 edges are left, 5 of them between basal ganglia and cortical areas.

Table 3
Connections between indicated areas in patients, related to duration of symptoms corrected for age at examination, in Pearson's correlation calculated between individual ROIs by SSPS (CC: Correlation Coefficients, all without significance after FDR correction) and in NBS (T: NBS test statistics, all with significance threshold $p < 0.05$).

Connection	CC	T
Putamen L to Postcentral Gyrus L	−0.288	11.36
Putamen L to Pre-SMA L	0.632	11.92
Putamen L to Sup. Part of Cerebellum R	−0.227	9.20
Putamen R to Pre-SMA L	0.599	10.25
Putamen R to Pre-SMA R	0.536	12.37
Globus Pallidus L to Pre-SMA L	0.667	25.32
Caudatum R to Sup. Part of Cerebellum L	−0.372	13.09
Ventral Premot. Area L to Pre-SMA R	−0.258	8.99
Dorsal Premot. Area L to Pre-SMA L	−0.610	9.48
SMA L to SMA R	0.087	10.25
SMA R to Sup. Part of Cerebellum L	−0.233	19.00
Sup. Parts of Cerebellum, L to R	−0.037	15.65

controls).

At the threshold of $t = 0.4$, these connections were excluded completely, and 2 separate components remained: one cortical sub-network with 12 nodes in both groups, with 15 edges in patients and 17 edges in controls. The second component comprised a sub-network of the basal ganglia with 6 nodes each and 9 edges in patients as compared to 15 edges in controls.The significance of these results was convincingly high ($p < 0.001$) at all three thresholds.

Network comparison between younger and older patients in different stages of disease progression did not show significant differences.

3.2. Correlation of CCs between motor-related areas and clinical data in patients

In patients, correlations of those CCs individually calculated between motor-related ROIs and clinical data were mostly negative. After FDR correction, none of them reached significance.

NBS analysis of covariance of these CCs and clinical data, corrected for age at examination, showed 12 edges between 13 nodes, which were significantly ($p < 0.05$) related to duration of disease at a threshold of $t = 8.2$, with reduction to 11 edges and 12 nodes in case of an elevation of the threshold of $t = 9.2$ (Fig. 3). In 5 of them, connections of basal ganglia to cortical areas were involved (Table 3). 7 of these connections correlated negatively to clinical data, but the rather high CCs of basal ganglia to pre-Supplementary Motor Areas were positive. No other clinical data related significantly to patients' CCs in NBS analysis.

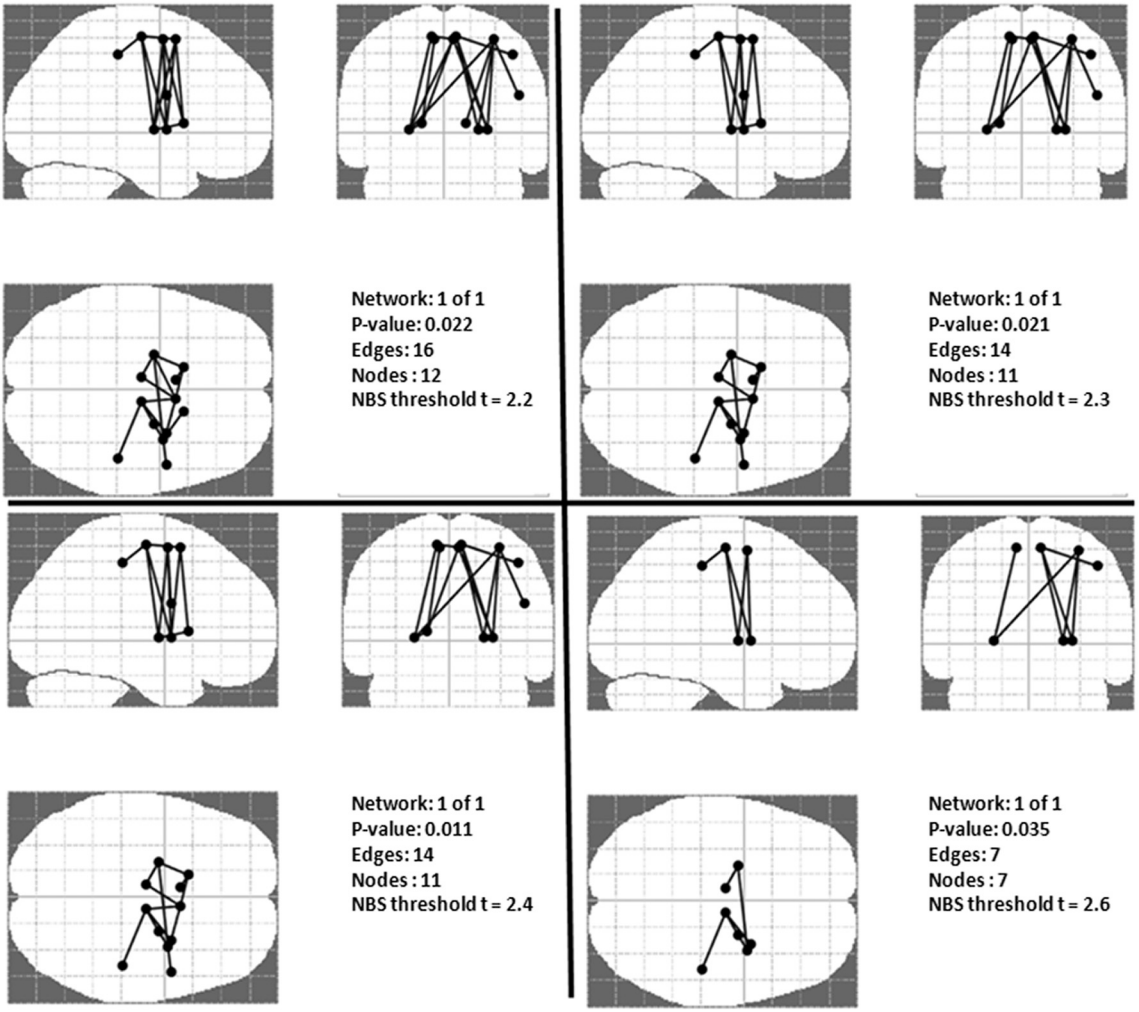

Fig. 4. NBS 2-tailed *t*-test results looking for differences between patients and controls at threshold levels of $t = 2.2$ (upper image left), $t = 2.3$ (upper image right), $t = 2.4$ (lower image left) and $t = 2.6$ (lower image right) showing between 12 nodes at lowest threshold and 7 nodes at highest threshold and between 16 and 7 edges. The edges, which -with 2 exceptions- are situated between basal ganglia and cortical ROIs, represent significant differences of inter-nodal edges between the group of patients and controls ($p < 0.05$).

Table 4
CCs of indicated areas, which are significantly ($p < 0.05$) different between patients and controls in NBS analysis. T-values of NBS *t*-test statistics comparing edges of motor network nodes at threshold 2.4.

Connection	CC Patients	CC Controls	T
Globus Pallidus L to SMA L	0.051 ± 0.185	0.259 ± 0.197	2.99
Globus Pallidus L to Dorsal Premotor Area R	0.052 ± 0.225	0.178 ± 0.193	3.24
Caudatum L to Pre-SMA L	0.19 ± 0.174	0.355 ± 0.158	2.58
Caudatum L to Pre-SMA R	0.068 ± 0.167	0.294 ± 0.193	3.26
Gl. Pallidus R to SMA R	0.109 ± 0.167	0.194 ± 0.189	2.67
Gl. Pallidus R to Dorsal Premotor Area R	0.072 ± 0.147	0.187 ± 0.195	2.90
Putamen R to SMA R	0.125 ± 0.243	0.318 ± 0.224	2.63
Putamen R to Dorsal Premotor Area R	−0.037 ± 0.271	0.230 ± 0.166	2.97
SMA R to Postcentral Gyrus R	0.224 ± 0.261	0.362 ± 0.176	2.61

3.3. Comparison of CCs from motor-related networks between patients and controls

NBS *t*-test evaluation looking for differences between groups at threshold levels between $t = 2.2$ and $t = 2.6$ showed between 12 and 7 nodes representing ROIs of the cortical and basal ganglia compartments and between 16 and 6 edges, which connected basal ganglia and cortical ROIs, with only 2 exceptions (see Fig. 4). All CCs, from which these differences between patients and controls were calculated, were lower in patients (Table 4). The greatest difference was seen in the connections between the left globus pallidus and the right dorsal premotor area and between the left caudatum and the right pre-Supplementary Motor Area (SMA) with NBS statistical values of $T = 3.24$ and $T = 3.26$ at a threshold of $t = 2.4$. Results were significant ($p < 0.05$) at all thresholds, being highest at the 0.4-threshold ($p = 0.011$).

4. Discussion

To our knowledge this is the first report about an analysis of CCs of regional activity of the motor system during resting state in PKAN dystonia. These CCs are supposed to measure connectivity between selected ROIs, because correlations and anti-correlations of regional BOLD signal time courses may be regarded as a measure of functional connections [21].

We decided to apply NBS in our network analysis, because we were especially interested in connectivity between basal ganglia and globus pallidus as the site of the primary lesion, as well as other motor system-related centers. In contrast to analysis of topological organization as measurement of small-worldness, efficiency, characteristic path length etc., which express the pattern of interplay between connections at a more global level, NBS deals with pairwise connectivity of brain regions. Thus, NBS can yield substantially greater statistical power than generic procedures to identify sub-networks in which the connectivity shows significant between-group difference [22]. We used various thresholds, because threshold definition is an important factor to influence number of primary selected significant network connections and their between-group differences. However, the choice of this primary threshold in NBS affects only the sensitivity of the method, but not the validity of family wise error correction [19].

The main result of this study is the demonstration of a significantly lower functional connectivity within the motor system in dystonic patients as compared to normal controls, especially between the basal ganglia and the motor-related cortical areas. The fact that nearly half of all connections, which were significantly correlated to duration of disease, were connections between basal ganglia and cortical areas and not connections within one of the sub-systems, underlines the crucial role of these connections for functionality of the motor system.

Previous reports about connectivity during resting state in other forms of dystonia as focal or task-specific dystonia provided contradictive results: As a common feature of musician's and laryngeal dystonia, a disorganization of its network kernel has been proposed, leading to abnormal sensorimotor processing in laryngeal dystonia and motor control management in hand dystonia. Musician's dystonia was characterized by "aberrant interactions between sensory and motor execution systems", and dystonic non-musicians showed "abnormal integration of sensory feedback into motor planning and executive control" [23]. This network kernel disorganization was accompanied by larger-scale abnormalities of connectivity. Some authors found reduced connectivity in the sensorimotor system as in cervical dystonia with partial normalization after Botox treatment [24], focal hand dystonia, blepharospasm, or spasmodic dysphonia [25]. Others saw mixed results as a bilateral increase of connectivity in the mouth area contrasting to a reduction in other parts of the sensorimotor system in brouchure dystonia [26], an increase between basal ganglia, in some cases combined with a decrease in the left postcentral area as well as elevations and reductions on different sides of this system, in writer's cramp [27].

In primary dystonia, which resembles the clinical picture of PKAN, symptomatic DTY1 carriers showed increased connectivity of the sensorimotor system, which affected its integration into posterior parietal networks [28]. A mouse model of Primary Type 1 Dystonia however revealed increased functional connectivity across the striatum, thalamus, and somatosensory cortex and reduced functional connectivity in the motor and cerebellar cortices [29]. Results of structural and functional Positron Emission Tomography and MRI studies are consistent with the concept of a circuit disorder involving cortico-striatal-pallido-thalamo-cortical and cerebello-thalamo-cortical pathways [30].

It has been proposed that the hyperactivation of the motor system, also described in PKAN [8], may be due to a reduced feed-back inhibition, a sensorimotor dysbalance and/or a generalized hyper-plasticity with a reduced capability to maintain homeostasis [31]. This view is in line with the concept of a "complex motor network rather than a limited disruption of individual nuclei in the basal ganglia" [32]. The concept has been substantiated by tractographic results and has been used to identify targets for deep brain stimulation in Parkinson's disease and dystonia [33–35].

According to neuropathologic and MRI findings as outlined above, globus pallidus is the first and main nucleus of the basal ganglia to be affected in PKAN, and the resulting reduction of its inhibitory input to the motor nucleus of the thalamus is the traditional pathophysiologic concept to "explain" the origin of dystonic movements in PKAN [9]. However, according to our study, the correlation coefficients of activity between these nuclei during rest are not significantly different from normal, in contrast to the significant deviations of correlations between the cortical motor-related areas and the basal ganglia, and this finding may point to a more general disconnection within the motor system.

Our results of a decreased connectivity are more in line with findings in early stages of Parkinson's disease, where hyperactivation of task-related areas during working memory processing went along with a reduced inter-regional connectivity [36]. The hyperactivation has been interpreted as a compensatory mechanism [37]. This might as well apply to the hyperactivity described during motor activation in PKAN patients in a previous study [8].

From a structural point of view, there are some reports about more widespread abnormalities in PKAN patients, which as well are in favor of a more general alteration in this type of dystonia and not just confined to the lesion known as the "tiger's eye": Voxel based morphology analysis showed increased grey matter density in the striatum, but also in the anterior cingulated cortex in children, which regressed during older age [38]. In white matter, patients showed reductions of fractional anisotropy mainly in the frontal lobes, the anterior branches of the internal capsules and in the surroundings of the third ventricle [39].

Due to the main limitation of the present study, the rather small sample size and the high heterogeneity of duration and clinical expression of the disease, we were not able to analyze connectivity between basal ganglia and other centers of the motor network in more detail in order to confirm or exclude a change of connectivity especially of the affected globus pallidus, as has been done before by connectivity-based parcellation [40]. Thus, comparisons of connectivity between individual nuclei by Pearson's correlation analysis corrected for age, did not show significant differences between groups, and NBS does not allow for single correlation analysis. However, the more general view of the motor network model as the anatomical basis of dystonia is supported by this functional study of resting state connectivity.

5. Conclusion

The finding of a reduced functional connectivity within the motor network, mainly between the basal ganglia and cortical motor-related areas, fits well into the concept of a general functional disturbance of the motor system in PKAN. This hypothesis is supported by previous reports about more widespread structural alterations not just confined to globus pallidus and resembles pathophysiologic concepts in other forms of dystonia.

Declaration of Competing Interest

No conflicts of interest have been declared by the authors.

Acknowledgments

The authors like to thank CEDIMAT and the Dr. Juan Taveras Foundation for generously supporting the PKAN project in the Dominican Republic.

References

[1] S.J. Hayflick, S.K. Westaway, B. Levinson, et al., Genetic, clinical, and radiographic delineation of Hallervorden-Spatz syndrome, N. Engl. J. Med. 348 (2003) 33–40.
[2] V. Leoni, L. Strittmatter, G. Zorzi, et al., Metabolic consequences of mitochondrial coenzyme A deficiency in patients with PANK2 mutations, Mol. Genet. Metab. 105 (2012) 463–471.
[3] P.S. Bindu, S. Desai, K.E. Shehanaz, M. Nethravathy, P.K. Pal, Clinical heterogeneity in Hallervorden-Spatz syndrome: a clinicoradiological study in 13 patients from South India, Brain Dev. 28 (2006) 343–347.
[4] M.C. Kruer, M. Hiken, A. Gregory, et al., Novelhistiopathologic findings in molecularly-confirmed pantothenate kinase-associated neurodegeneration, Brain 134 (2011) 947–958.

[5] S.J. Hayflick, M. Hartman, J. Coryell, J. Gitschier, H. Rowley, Brain MRI in neurodegeneration with brain iron accumulation with and without PANK2 mutations, AJNR Am. J. Neuroradiol. 27 (2006) 1230–1233.
[6] C. Vilchez-Abreu, P. Roa-Sanchez, R. Fermin-Delgado, et al., El signo del "Ojo del Tigre" en resonancia magnética: cambios relacionados con la edad, Anal. Radiol. Mexico 3 (2013) 189–196.
[7] P. Roa, P. Bido, B. Foerster, et al., Evaluation of the "Tiger's Eye" by quantitative susceptibility imaging, ACR J. Radiol. Med. Imaging 2 (2017) 7–11.
[8] P. Stoeter, R. Rodriguez-Raecke, C. Vilchez, et al., Motor activation in patients with Pantothenate Kinase-Associated Neurodegeneration: a functional magnetic resonance imaging study, Parkinsonism Relat. Disord. 18 (2012) 1007–1010.
[9] J.W. Mink, The basal ganglia and involuntary movements: impaired inhibition of competing motor patterns, Arch. Neurol. 60 (2003) 1365–1368.
[10] A. Cacciola, A. Calamuneri, D. Milardi, et al., A Connectomic analysis of the human basal ganglia network, Front. Neuroanat. 11 (2017) 85 (eCollection 2017).
[11] J. Schiessl-Weyer, P. Roa, F. Laccone, et al., Acanthocytosis and the c.680 A>G mutation in the PANK2 gene: a study enrolling a cohort of PKAN patients from the Dominican Republic, PLoS One 10 (2015), e0125861.
[12] P. Roa, P. Stoeter, E. Perez-Then, M. Santana, R. Marshall, A pilot study of a potential phosphopantothenate replacement therapy in 2patients with pantothenate kinase-associated neurodegeneration, Int. J. Rare Dis. Orphan. Drugs 2 (2017) 1006–1012.
[13] M.A. Mayka, D.M. Corcos, S.E. Leurgans, D.E. Vaillancourt, Three-dimensional locations and boundaries of motor and premotor cortices as defined by functional brain imaging: a meta-analysis, Neuroimage 3 (2006) 1453–1474.
[14] W.R. Shirer, S. Ryali, E. Rykhlevskaia, V. Menon, M.D. Greicius, Decoding subject-driven cognitive states with whole-brain connectivity patterns, Cereb. Cortex 22 (2012) 158–165.
[15] J. Goñi, M.P. van den Heuvel, A. Avena-Koenigsberger, et al., Resting-brain functional connectivity predicted by analytic measures of network communication, Proc. Natl. Acad. Sci. U. S. A. 111 (2014) 833–838.
[16] K. Murphy, M.D. Fox, Towards a consensus regarding global signal regression for resting state functional connectivity, MRI Neuroimage 154 (2017 Jul 1) 169–173.
[17] J.D. Power, K.A. Barnes, A.Z. Snyder, B.L. Schlaggar, S.E. Petersen, Spurious but systematic correlations in functional connectivity MRI networks arise from subject motion, Neuroimage 59 (2012) 2142–2154.
[18] J. Wirsich, A. Perry, B. Ridley, et al., Whole-brain analytic measures of network communication reveal increased structure-function correlation in right temporal lobe epilepsy, Neuroimage Clin. 11 (2016) 707–718.
[19] A. Zalesky, A. Fornito, E.T. Bullmore, Network-based statistic: identifying differences in brain networks, Neuroimage 53 (2010) 1197–1207.
[20] C. Zhan, H.J. Chen, Y.Q. Gao, T.X. Zou, Functional network-based statistics reveal abnormal resting-state functional connectivity in minimal hepatic encephalopathy, Front Neurol. 10 (2019 Jan 29) (33eCollection 2019).
[21] S. Achard, R. Salvador, B. Whitcher, J. Suckling, E. Bullmore, A resilient, low-frequency, small-world human brain functional network with highly connected association cortical hubs, J. Neurosci. 26 (2006) 63–72.
[22] E. Bullmore, O. Sporns, Complex brain networks: graph theoretical analysis of structural and functional systems, Nat. Rev. Neurosci. 10 (2009) 186–198.
[23] S. Fuertinger, K. Simonyan, Task-specificity in focal dystonia is shaped by aberrant diversity of a functional network kernel, Mov. Disord. 33 (2018) 1918–1927.
[24] C.C. Delnooz, J.W. Pasman, C.F. Beckmann, B.P. van de Warrenburg, Altered striatal and pallidal connectivity in cervical dystonia, Brain Struct. Funct. 220 (2015) 513–523.
[25] G. Battistella, S. Fuertinger, L. Fleysher, L.J. Ozelius, K. Simonyan, Cortical sensorimotor alterations classify clinical phenotype and putative genotype of spasmodic dysphonia, Eur. J. Neurol. 23 (2016) 1517–1527.
[26] B. Haslinger, J. Noé, E. Altenmüller, et al., Changes in resting-state connectivity in musicians with embouchure dystonia, Mov. Disord. 32 (2017) 450–458.
[27] T. Mantel, T. Meindl, Y. Li, A. Jochim, et al., Network-specific resting-state connectivity changes in the premotor-parietal axis in writer's cramp, Neuroimage Clin. 17 (2017) 137–144 (eCollection 2018).
[28] E. Premi, M. Diano, S. Gazzina, et al., Functional connectivity networks in asymptomatic and symptomatic DYT1 carriers, Mov. Disord. 31 (2016) 1739–1743.
[29] J.C. DeSimone, M. Febo, P. Shukla, et al., In vivo imaging reveals impaired connectivity across cortical and subcortical networks in a mouse model of DYT1 dystonia, Neurobiol. Dis. 95 (2016) 35–45.
[30] M. Carbon, D. Eidelberg, Abnormal structure-function relationships in hereditary dystonia, Neuroscience 164 (2009) 220–229.
[31] A. Quartarone, V. Rizzo, S. Bagnato, et al., Homeostatic-like plasticity of the primary motor hand area is impaired in focal hand dystonia, Brain 128 (2005) 1943–1950.
[32] D. Milardi, A. Quartarone, A. Bramanti, et al., The cortico-basal ganglia-cerebellar network: past, present and future perspectives, Front. Syst. Neurosci. 13 (2019 Oct 30) 61 (eCollection 2019).
[33] W.J. Neumann, A. Jha, A. Bock, et al., Cortico-pallidal oscillatory connectivity in patients with dystonia, Brain 138 (Pt 7) (2015 Jul) 1894–1906.
[34] W.J. Neumann, A. Horn, S. Ewert, et al., A localized pallidalphysiomarker in cervical dystonia, Ann. Neurol. 82 (6) (2017 Dec) 912–924.
[35] A. Quartarone, A. Cacciola, D. Milardi, et al., New insights into cortico-basal-cerebellar connectome: clinical and physiological considerations, Brain 143 (2) (2020 Feb 1) 396–406.
[36] Gerrits N.J.H.M. TrujilloJP, D.J. Veltman, H.W. Berendse, Y.D. van der Werf, O. A. van den Heuvel, Reduced neural connectivity but increased task-related activity during working memory in de novo Parkinson patients, Hum. Brain Mapp. 36 (2015) 1554–1566.
[37] C.C. De Bondt, N.J.H.M. Gerrits, D.J. Veltman, H.W. Berendse, O.A. van den Heuvel, Y.D. van der Werf, Reduced task-related functional connectivity during a set-shifting task in unmedicated early-stage Parkinson's disease patients, BMC Neurosci. 17 (2016) 20–31.
[38] R. Raecke, P. Roa-Sanchez, H. Speckter, et al., Grey matter alterations in patients with Pantothenate Kinase-Associated Neurodegeneration (PKAN), Parkinsonism Relat. Dis. 20 (2014) 975–979.
[39] P. Stoeter, P. Roa-Sanchez, H. Speckter, et al., Changes of cerebral white matter in patients suffering from Pantothenate Kinase-Associated Neurodegeneration (PKAN): a Diffusion Tensor Imaging (DTI) study, Parkinsonism Relat. Disord. 21 (2015) 577–581.
[40] S. Bertino, G.A. Basile, A. Bramanti, et al., Spatially coherent and topographically organized pathways of the human globus pallidus, Hum. Brain Mapp. 41 (2020) 4641–4661.